Materials Physics and Mechanics. 2023;51(6): 24-41
Research article
http://dx.doi.org/10.18149/MPM.5162023_3

Submitted: March 27, 2023
Approved: May 30, 2023
Accepted: June 20, 2023

Study on nanosized Al_2O_3 and Al_2O_3-SiC on mechanical, wear and fracture surface of Al7075 composites for soil anchoring applications

M. Ravikumar [1] ✉, R. Naik [1], B.R. Vinod [2], K.Y. Chethana [1], Y.S. Rammohan [1]

[1] BMS College of Engineering, Karnataka, India

[2] BMS Institute of Technology and Management, Karnataka, India

✉ ravikumar.muk@gmail.com

Abstract. Mechanical and tribological tests of aluminium 7075 alloy, mono-composite (Al7075 + 1 % Al_2O_3), and hybrid composite (Al7075 + 1 % Al_2O_3 + 1 % SiC) have been performed in this study according to ASTM standards. Through the stir casting process, mono and hybrid composite materials were prepared. It was discovered that adding more hard ceramic particles improved hardness and strengthened tensile strength. In contrast to Al7075 alloy, hybrid MMCs enhanced tensile strength and superior hardness. The obtained results indicate that highest hardness of 78 VHN and tensile strength of 126 MPa were achieved for developed hybrid composites. A pin-on-disc wear test rig was used to conduct wear experiments. The Taguchi approach was used to optimise the wear parameters. The findings showed that the load had a greater impact on the wear behaviour of Al7075 alloys than did sliding distance and speed. The wear behaviour in mono composites and hybrid composites was improved by the addition of nano sized Al_2O_3 and SiC particulates to Al7075. Improved wear resistance for monolithic, mono and hybrid composites was achieved at 5 N of load, 100 rpm of speed and 250 m of sliding distance. Abrasion and adhesion-related damages were discovered by micrograph studies. Flows with the deep grooves were observed on the worn-out surface of mono composite. It provided the evidence of the mono composites' abrasive mechanism. Comparing the hybrid MMCs to the monolithic and mono composite MMCs it was seen that, the hybrid composites (Al7075 + 1 % Al_2O_3 + 1 % SiC) exhibited better wear resistance.

Keywords: Al7075; Al_2O_3/Al_2O_3-SiC; mechanical behavior; wear behavior; fracture analysis; Taguchi technique

Acknowledgements. *The authors are very thankful to Dr. R Suresh, Professor, Department of Mechanical and Manufacturing Engineering, M S Ramaiah University of Applied Sciences for continuous support in completion of this research work.*

Citation: Ravikumar M, Naik R, Vinod BR, Chethana KY, Rammohan YS. Study on nanosized Al_2O_3 and Al_2O_3-SiC on mechanical, wear and fracture surface of Al7075 composites for soil anchoring applications. *Materials Physics and Mechanics.* 2023;51(6): 24-41. DOI: 10.18149/MPM.5162023_3.

Introduction

From the last few decades, due to their superior mechanical properties compared to the basic materials, light metal matrix composites (MMCs) materials with ceramic reinforcement particles have drawn a lot of focus in recent years [1]. The aluminium (Al) alloy composites are mainly used for several functional applications like agriculture mechanization, soil anchoring and building structures due to their high strength, lightweight design, high wear resistance, better thermal and electrical conductivity, excellent castability, and strengthening using precipitation hardening [2]. These alloys restrict the materials' ability to be used for

Publisher: Peter the Great St. Petersburg Polytechnic University

functional purposes because of their moderate hardness, low elastic modulus, and low temperature properties. By incorporating various ceramic strengthening particles into the matrix of the Al alloy, it is saturated. The Al metals used in soil anchoring applications is Al7075. Increased stiffness, strength, better wear resistance, and excellent thermal conductivity were all added by the hard particulate reinforcement. Al_2O_3, SiC, B_4C, TiB_2, TiO_2, ZrO_2, Si_3N_4, Gr, TiC, and MgB_2 are used as supports. Al_2O_3, ZrO_2, SiC, and Gr [3] are the most frequently used reinforcing materials. Composites made from silicon carbide and aluminium oxide could be used in a variety of engineering disciplines. Al_2O_3-SiC is now particularly well suited for ballistic protection equipment, rockets engine nozzle throats, space shuttle surface tiles, piston crowns and cylinders, nose cones of hypersonic re-entry vehicles, and the harp shaped structures of hypersonic rocket engines. Because SiC dispersoids prevent the Al_2O_3 matrix's grain development, the reinforcement of SiC particles in the Al matrix produces better mechanical, wear, physical and interfacial properties. The pre-processing, post-processing, and production techniques, in addition to the reinforcement, significantly improve the properties. In their study of the mechanical and tribological properties of Al-Al_2O_3 composites, Kumar et al. [4] found that while elongation decreases, alloy composites' tensile strength, toughness, and wear resistance increase. In their analysis of the wear characteristics of AA356/Al_2O_3 composites, Alhawari et al. [5] found that the wear rate reduces as the weight fraction of Al_2O_3 particulates rises. The physical and mechanical properties of AA356/Al_2O_3 composites with the inclusion of micro and nanosized Al_2O_3 particulates were investigated by Sajjadi et al. [6]. They noticed that porosity and hardness increased with weight percentage and decreased with Al_2O_3 particulate size. Al_2O_3 has a significant influence on the tensile strength and hardness of the welded joint, according to research by B.M. Nagesh et al. on the effects of weld parameters on AA 6082 reinforced with Al_2O_3 at three different weight percentages (5, 10, and 15 wt. %) [7]. Reddy et al. [8] analysis of the tensile properties of AA356/SiC nanocomposites revealed a notable rise in performance with increasing SiC nanoparticle content. The microstructural, mechanical, and tribological properties of Al/SiC alloys were investigated by Ghandvar et al. [9]. They discovered that adding 25 wt. % SiC particulates increased hardness, whereas adding 20 wt. % SiC particulates increased wear resistance in metal composites. The mechanical properties of the AA356 alloy reinforced with nano and micro SiC particulates were researched by Amouri et al. [10]. When nano-SiC particles up to 1.5 wt. % were added, they discovered improvements in the mechanical properties. Using pin-on-disc equipment, Shivmurthy et al. [11] investigated the tribological behaviour of AA356/SiC composites. They discovered that compared to other proportions, 10 vol. % SiC particles exhibit a lower rate of wear. The survey that was previously described shows the mechanical and tribological characteristics of composites with various ceramic particles. However, little attention has been paid to the wear and mechanical properties of composite reinforced with hard ceramic particles under the various process circumstances. In this investigation, the mechanical characteristics and wear patterns of mono and hybrid MMCs made of Al7075 alloy were examined. The findings of the present study demonstrate how two distinct reinforcements influence mechanical behaviour. In order to analyse the wear behaviour of MMCs, numerous parameters and factors, such as speed (rpm), load (N), and sliding distance (m), were taken into account. The results were then compared to the optimized values. In order to evaluate the worn surfaces of test materials, SEM analysis was used.

Materials and Method

As the base material, Al alloy 7075 was utilized. It has superior fracture toughness, wear, and corrosion resistance. It is widely employed in automobiles and aerospace field. Al7075's material compositions are shown in Table 1 as a weight percentage. Nano sized (50 nm) SiC

and Al_2O_3 with a pH value of 6.5 to 7.5 were used as reinforcing materials. In this study, two different MMC types such as mono composite (Al7075 + 1 % Al_2O_3) and hybrid composites (Al7075 + 1 % Al_2O_3 + 1 % SiC) were produced and compared to Al7075. Both types of composites, mono and hybrid MMCs, were produced utilising stir casting method in a coke furnace. To prevent particle aggregation, stirring was carried out using a 4-blade stirrer for a total of 5 minutes at an average speed of 250 rpm. A graphite crucible was used to melt the base alloy. The pre-heated nano sized Al_2O_3 and SiCp were mixed into the ready molten melt while stirring. Inert gases existing in the molten metal were removed using a degasifying tablet. The pre-heated mould box was filled with molten composite melt. Finally, a CNC lathe was used to machine the composite materials. Composite specimens with various cross sections were constructed for the microstructure analysis, and they were polished with diamond paste on emery paper with a 400 grit size. Finally, in accordance with the procedure for a metallographic examination, test specimens were then polished by using velvet cloth disk polishing apparatus to provide a satisfactory finish on the test sample surface.

Table 1. Composition of Al 7075 with wt. %

Content	Zn	Mg	Cu	Si	Fe	Ni	Mn	Sn	Cr	Al
Wt. %	5.42	2.30	1.48	0.06	0.25	0.05	0.05	0.01	0.28	Remaining

Result and the Discussions

Microstructural analysis. The microstructure of Al7075, mono-composites (Al7075 + 1 % Al_2O_3), and hybrid composites (Al7075 + 1 % Al_2O_3 + 1 % SiC) is depicted in Fig. 1. The monolithic micrograph image shown in Fig. 1(a) demonstrates the presence of intermetallic complexes. A mono composite with a uniform Al_2O_3 particle dispersal in the Al alloy matrix material is shown in Fig. 1(b). Typically, this is attributable to the precise stirring method used during production. The micrographs in Fig. 1(c) show homogeneous dispersion of Al_2O_3-SiC particles in hybrid composites. We can see that the alloy's reinforced particles are dispersed at random. However, at several locations the particulates are seen to be clumping together. Other researchers also got comparable outcomes [12–15]. Due to a rise in the weight percentage of hard particles in the hybrid MMCs, particle aggregation increased in several areas.

Hardness. According to ASTM-E92 standards, the microhardness of Al7075, mono MMCs (Al7075 + 1 % Al_2O_3), and hybrid MMCs (Al7075 + 1 % Al_2O_3 + 1 % SiC) were examined. Under a steady load of 2 kg, a diamond shaped 10 mm indenter was used. Three separate locations on the test samples were evaluated for their hardness. The average hardness value was then noted. Figure 2 shows the microhardness for each composition. When compared to monolithic, the hardness values of the mono composites and hybrid composites are higher, as can be shown in Fig. 2. The base matrix's base matrix is more tightly coupled and evenly distributed with the hard ceramic particles. Therefore, as the dislocations come into contact with these tough ceramic particles, additional tension is necessary for movement. Therefore, better dispersion strengthening through proper particles dislocation interaction may be responsible for the uniform distribution of hard ceramic particles [16–18]. Since Al_2O_3 and SiC are two separate hard ceramic particles, the MMCs reinforced with them have improved hardness.

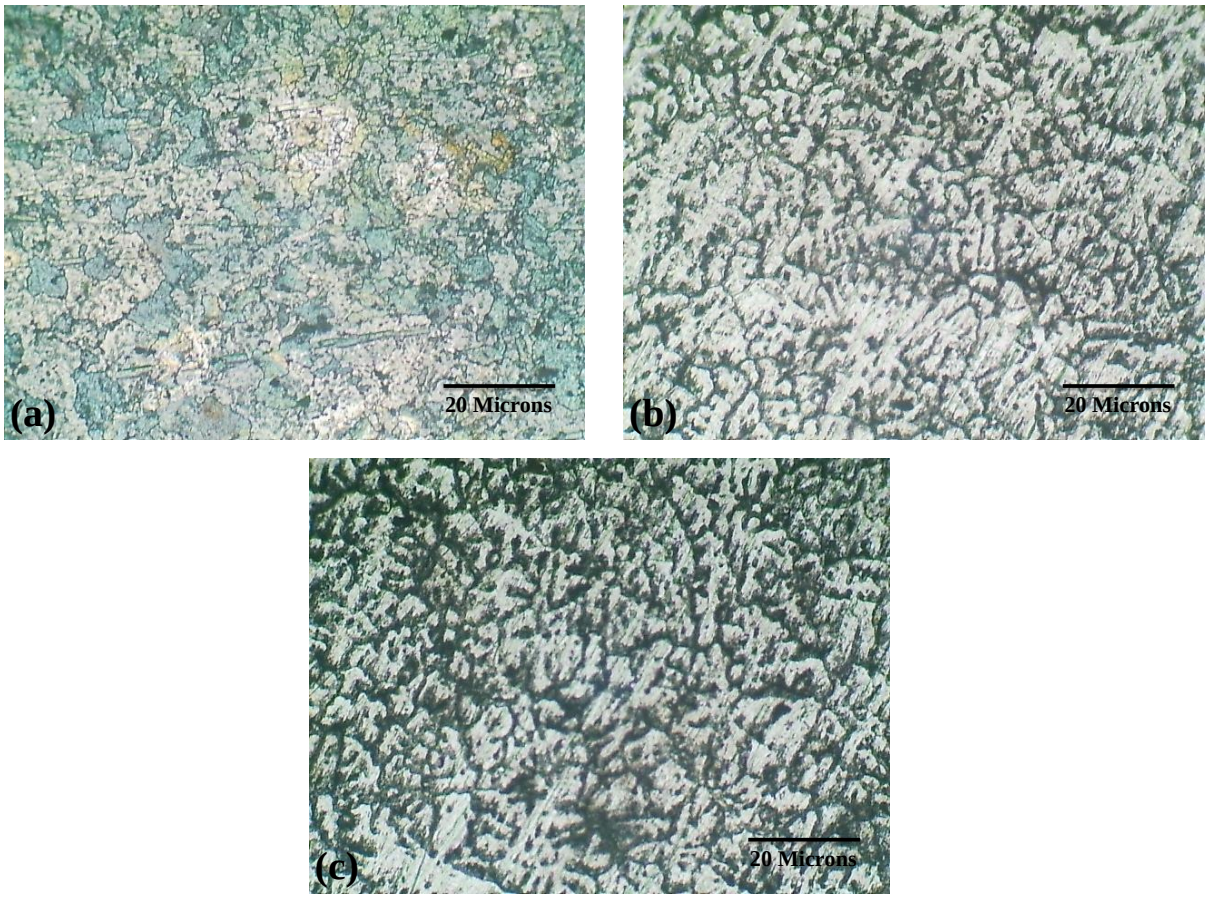

Fig. 1. Micro-structure of (a) monolithic, (b) mono MMCs (Al7075 + 1% Al_2O_3) and (c) hybrid MMCs (Al-7075 + 1% Al_2O_3 + 1% SiC)

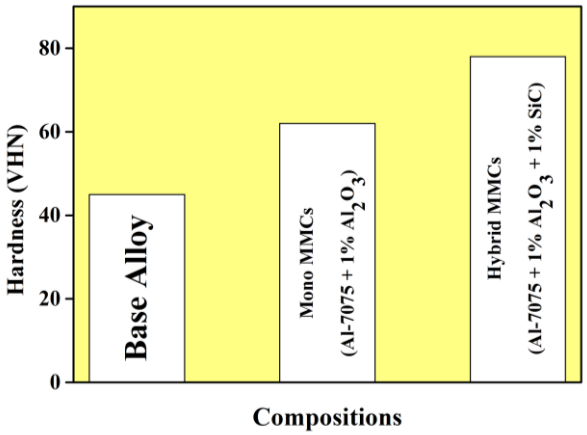

Fig. 2. Microhardness of base alloy, mono and the hybrid MMCs

Tensile behavior. Tensile tests trials were carried out utilising UTM at a maximum loading capacity of 450 KN in accordance with ASTM-E8 regulations. In the current study, three test samples with comparable compositions were examined to determine the average tensile strength. The values' fluctuation in this instance was under 5 %. Figure 3(a) displays the tensile strength findings for each mixture. When compared to monolithic and mono MMCs, the hybrid MMCs have higher tensile strengths. Results show that the tensile strength is enhanced by adding more hard ceramic particles. Enhancement in tensile strength is due to the addition of hard nano sized Al_2O_3 particles in mono composites and nano sized Al_2O_3 + SiC in hybrid MMCs, which enhanced the tensile strength. Enhancement in tensile

strength could also be attributed to the uniform particle dispersion and reduced porosity found in composite and hybrid MMCs. This finding is consistent with the outcomes of the majority of Al composites reinforced with hard ceramic particulates [16,17,19]. In Fig. 3(b), the stir casting method's composite samples' tensile stress-strain curves are displayed. For monolithic, mono-composites, and hybrid-composites, a stress-strain diagram is drawn. The primary characteristics of this graph are that the fracture strain decreases with increasing particle content, and the tensile strength rises in response. In comparison to mono-composite and hybrid-composites, the monolithic alloy is found to have the largest plastic strain and the least resistance to plastic deformation due to its relatively lower flow stress. It has been found that all MMCs offer increased strength above the basic alloy. The grain refining and particle strengthening are the main reasons for this development. Al_2O_3 and SiC, two hard ceramic nanoparticles, strengthen the composite to enable it to endure greater stresses. The graph of the stress-strain curve shown in Fig. 3(b) also shows that a hybrid composite containing 1 % nanoscale Al_2O_3 and 1 % nanoscale SiC particulates can bear the highest stress. The stress-strain curve shows that in addition to strong tensile strength, the toughness has improved. This matters a lot. Meanwhile, ductility is reduced by the majority of ways for increasing strength.

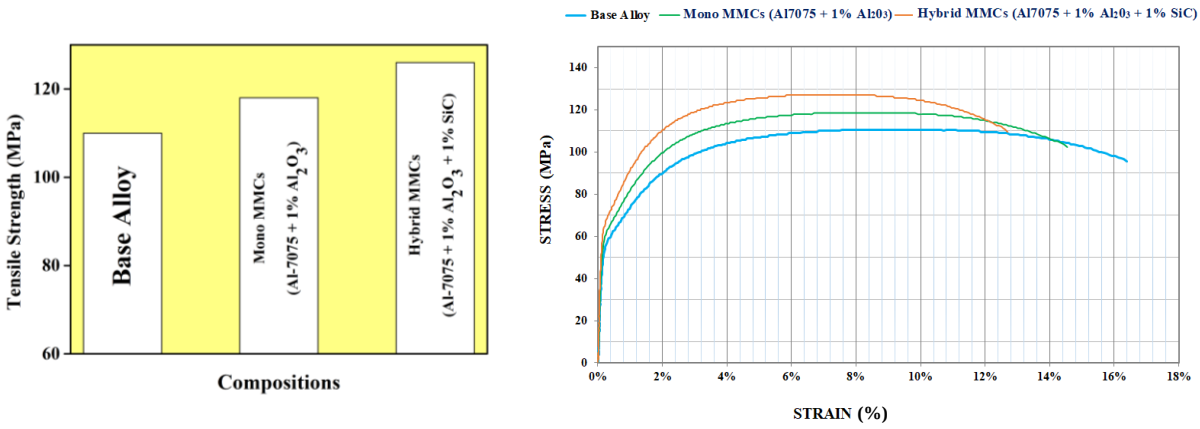

(a) (b)

Fig. 3. Tensile strength (a) and stress-strain curves (b) of base alloy, mono and hybrid MMCs

A Scanning Electron Microscope (SEM) is used to examine the newly formed crack surface that was produced by the fracture test. After conducting the test, Fig. 4(a) depicts the shattered surface of the base material, Fig. 4(b) the fractured surface of mono composites, and Fig. 4(c) the fractured surface of hybrid composites. Surface analysis showed that the fracture occured in both transgranular and intergranular types of fracture, combining broken particles, pulled regions, and tiny plastic dimples to produce mixed mode fracture, which has high strength prior to fracture. Fracture surfaces for the composites and hybrid MMCs containing nano sized Al_2O_3 and SiC particles displayed various topographies. The majority of the dimples on the shattered surface, according to a close inspection, were connected to the matrix material. Large dimples and a significant degree of plastic deformation were found as a result of shattered surface analysis performed on fracture toughness specimens of FCC structured Aluminum alloy samples, indicating ductile fracture (ref Fig. 4(a)). The fractured surface shows that the matrix material is primarily represented by the fractured particles, which indicates ductile fracture. Due to the presence of too many nanoparticles, the fracture surface of mono composites (ref. Fig. 4(b)) reveals mixed mode fracture, while hybrid composites (ref. Fig. 4(c)) reveals cleavage type fracture. Also, it should be highlighted that clustered particles are vulnerable to early composite degradation, and large particles appear to be more likely to fracture, which resulted in a decrease in the fracture toughness value [20,21].

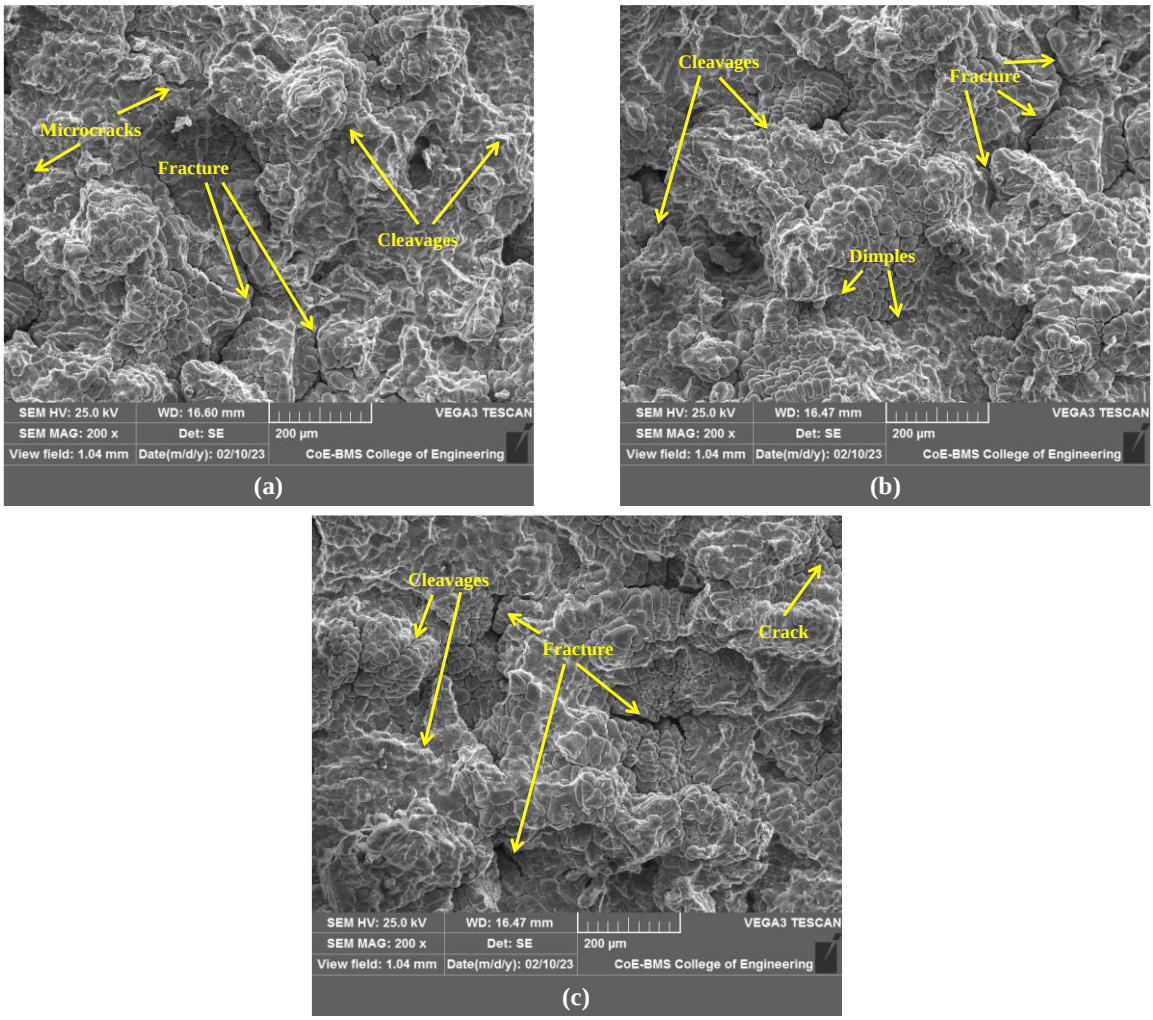

Fig. 4. Fracture surface of (a) monolithic, (b) mono and (c) hybrid MMCs

Based on the literature review and preliminary experimentation conducted by the authors, the research work is carried out on the effect of monolithic, mono and hybrid reinforcement on mechanical and wear properties in Al7075 were studied. The obtained results indicated that, the effect of nano sized 1 % Al_2O_3 + 1 % SiC reinforcements on mechanical and wear properties in Al7075 hybrid composites is more when compared to the monolithic and mono composites. So, the strengthening effect in hybrid composite is more compared to monolithic and mono composites because of synergistic properties were obtained more in hybrid composites.

Experimenting with wear behaviour using the Taguchi method. This method is a potent design concept that is frequently used in many different industries [22,23]. It is frequently developed to provide superior goods at a lesser price. It is typically used to analyse the effects of varrying the parameters. Testing was carried out on the test samples utilising Taguchi evaluation of the L27 orthogonal array at room temperature (27 °C) (OA). Wear test specimens were produced using the ASTMG99 size of 6 mm in diameter and 30 mm in length. During the wear tests, the test specimens were firmly pressed against the hard rotating steel disc. After every trial, the disc and test samples were carefully cleaned with an organic chemical (acetone) to ensure the correctness of the results. The current experiment evaluates the wear behaviour as a loss of weight (gm) of a test material. The specimens were frequently cleaned with acetone solution before being weighed on a digital scale to ensure an accuracy of 0.0001 gm throughout the studies. The test specimens were cleaned, and the final weight was accurately measured. Wear loss was evaluated by considering the difference between initial and final weight of the test samples. Test trials were conducted on the basis of factors that

were selected and respective levels, which are shown in Table 2. Using samples of Al7075, mono MMCs (Al7075 + 1 % Al_2O_3), and hybrid MMCs (Al7075 + 1 % Al_2O_3 + 1 % SiC), 27 orthogonal array (OA) tests were performed. The findings are given in Table 3.

Table 2. Process parameters and levels

Sl. No.	Parameters	Levels	Levels	Levels
1	Load, N	5	7.5	10
2	Sliding Speed, rpm	100	300	500
3	Sliding Distance, m	250	500	750

Table 3. Taguchi L27 Orthogonal Array and their outcomes

Trial No.	Load, N	Sliding Speed, rpm	Sliding Distance, m	Wear loss, g		
				Monolithic	Mono MMCs (1 % Al_2O_3)	Hybrid MMCs (1 % Al_2O_3 + 1 % SiC)
1	5.0	100	250	0.030	0.020	0.010
2	5.0	100	500	0.040	0.025	0.015
3	5.0	100	750	0.050	0.035	0.020
4	5.0	300	250	0.040	0.020	0.010
5	5.0	300	500	0.040	0.023	0.015
6	5.0	300	750	0.060	0.035	0.025
7	5.0	500	250	0.056	0.030	0.010
8	5.0	500	500	0.065	0.037	0.020
9	5.0	500	750	0.070	0.040	0.030
10	7.5	100	250	0.050	0.025	0.012
11	7.5	100	500	0.070	0.045	0.033
12	7.5	100	750	0.075	0.055	0.040
13	7.5	300	250	0.060	0.047	0.020
14	7.5	300	500	0.070	0.055	0.037
15	7.5	300	750	0.075	0.060	0.045
16	7.5	500	250	0.055	0.035	0.021
17	7.5	500	500	0.065	0.040	0.030
18	7.5	500	750	0.065	0.050	0.032
19	10.0	100	250	0.050	0.035	0.015
20	10.0	100	500	0.050	0.035	0.025
21	10.0	100	750	0.070	0.045	0.030
22	10.0	300	250	0.070	0.050	0.040
23	10.0	300	500	0.075	0.060	0.030
24	10.0	300	750	0.079	0.065	0.055
25	10.0	500	250	0.081	0.070	0.045
26	10.0	500	500	0.085	0.075	0.060
27	10.0	500	750	0.089	0.080	0.065

Table 4. ANOVA outcomes of monolithic material

Parameters	DoF	Seq. S S	Adj. S S	Adj. M S	F-Values	P-Values	Contri-bution, %	Observation
Load, N	1	0.0021780	0.0021780	0.0021780	34.8894	0.0000051	36.89	Significant
Sliding speed, rpm	1	0.0011842	0.0011842	0.0011842	18.9700	0.0002321	20.06	Significant
Sliding distance, m	1	0.0011045	0.0011045	0.0011045	14.6930	0.0003367	18.71	Significant
Error	23	0.0014358	0.0014358	0.0000624			24.32	
Total	26	0.0059025					100	

R-Sq = 75.67 %

Table 5. ANOVA outcomes of mono MMCs

Parameters	DoF	Seq. S S	Adj. S S	Adj. M S	F-Values	P-Values	Contri-bution, %	Observation
Load, N	1	0.0034722	0.0034722	0.0034722	46.7095	0.0000006	48.17	Significant
Sliding speed, rpm	1	0.0010427	0.0010427	0.0010427	14.0270	0.0010567	14.46	Significant
Sliding distance, m	1	0.0009827	0.0009827	0.0009827	13.2199	0.0013828	13.63	Significant
Error	23	0.0017097	0.0017097	0.0000743			23.72	
Total	26	0.0072074					100	

R-Sq = 76.28 %

Table 6. ANOVA outcomes of hybrid MMCs

Parameters	DoF	Seq. S S	Adj. S S	Adj. M S	F-Values	P-Values	Contri-bution, %	Observation
Load, N	1	0.0024500	0.0024500	0.0024500	37.2366	0.0000032	40.31	Significant
Sliding speed, rpm	1	0.0007094	0.0007094	0.0007094	10.7817	0.0032566	11.67	Significant
Sliding distance, m	1	0.0014045	0.0014045	0.0014045	21.3464	0.0001199	23.11	Significant
Error	23	0.0015133	0.0015133	0.0000658			24.90	
Total	26	0.0060772					100	

R-Sq = 75.10 %

The ANOVA method, main effect plots, surface plots, linear regression, and normal probability graphs were used to examine the effects of process parameter changes. The "smaller is better" criteria was used for the study of wear loss in developed composites. Tables 4-6 show the results of the ANOVA for wear loss. P-values with a confidence level lower than 0.05 were deemed to have a substantial impact on performance [24, 25]. The main effects graph shown in Fig. 5 were used to verify the parameters' relevance. Table 4 displays the results of an ANOVA analysis of the wear parameters of the alloy Al 7075.

According to an ANOVA finding, the load (36.89 %) has a greater impact on wear loss than sliding speed (20.06) or distance (18.71). In contrast, the wear loss shown in Table 5 for Al7075 + 1 % Al_2O_3 is significantly influenced by load (N) (48.17 %), sliding speed (rpm) (14.46 %), and sliding distance (m) (13.63 %). However, the wear loss shown in Table 6 for developed hybrid Composite (Al7075/1 % Al_2O_3/ 1 % SiC) is significantly influenced by load (48.17 %), sliding distance (23.11) and sliding speed (14.46). The results show that the load is the most important relevant parameter for wear loss for all the developed composites, followed by the other two parameters. According to the outcomes, hard particles enable hybrid composites to have a lower wear rate than Al alloy and mono composite. Similar findings have been reported by several investigators [26]. The hard ceramic particulates protruding from the surface of the composites generate sharp asperities and produce uneven interaction between the counter-face and samples, which leads to increase wear rate. With the presence of secondary hard ceramic reinforcement, the distances between the particles in MMCs are close, resulting in the existence of more reinforcement phase. Hard reinforcing particles have been demonstrated to boost toughness in previous studies. It has been demonstrated that wear behaviour, material hardness, and wear loss are related [27]. When the increases in wear factor led to an increase in the wear loss, as can be observed in Fig. 5(a-c). Usually, the primary factor behind the outcomes is the formation of an oxide film on the matrix surface, which leads to increased wear. Hence, both a rise in temperature and a weakening of the composite surface lead to excessive wear. On the other hand, adding tough

particles makes mono MMCs more resistant to wear. As can be seen, the rapid sliding speed frequently increased wear loss and led to the delamination. Developed hybrid composites have better wear resistance than mono composite and monolithic materials [28, 29].

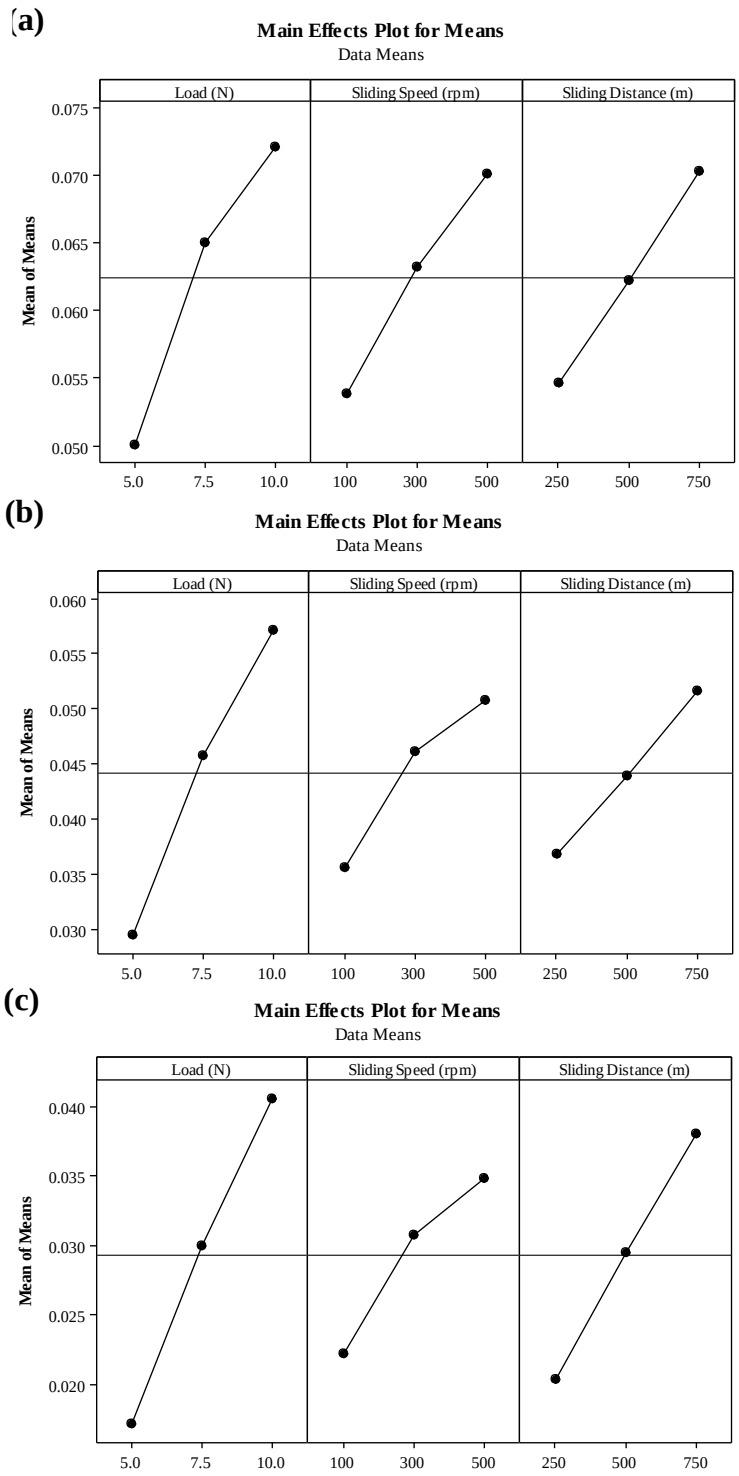

Fig. 5. Main Effects graphs for (a) monolithic, (b) mono MMCs and (c) hybrid MMCs

Based on rank given obtained to the mean points as depicted in Tables 7-9, the mean answer has been assessed. The variables are significant, and it is also clear that the load (N) which the delta of mean value placed as rank 1 and was followed by speed (rpm) and the sliding distance (m) for the aluminium alloy and developed composites is a significant factor.

Table 7. The response data for monolithic material

Levels	Load	Sliding speed	Sliding distance
1	0.05011	0.05389	0.05467
2	0.06500	0.06322	0.06222
3	0.07211	0.07011	0.07033
Delta	0.02200	0.01622	0.01567
Rank	1	2	3

Table 8. The response data for mono composites

Levels	Load	Sliding speed	Sliding distance
1	0.02944	0.03556	0.03689
2	0.04578	0.04611	0.04389
3	0.05722	0.05078	0.05167
Delta	0.02778	0.01522	0.01478
Rank	1	2	3

Table 9. The response data for hybrid composites

Levels	Load	Sliding speed	Sliding distance
1	0.01722	0.02222	0.02033
2	0.03000	0.03078	0.02944
3	0.04056	0.03478	0.03800
Delta	0.02333	0.01256	0.01767
Rank	1	3	2

Regression analysis uses a linear regression equation to illustrate the correlation between two or more predictor variables. The relationship between the wear factors and their interactions is established via a regression equation. Eqs. (1), (2), and (3), respectively, represent the regression analysis equations for matrix, mono, and the hybrid MMCs materials.

$$\textit{Wear rate of monolithic alloy} = 0.00157407 + 0.0044\ \textit{Load} + \\ + 4.05556e^{-005}\ \textit{Sliding speed} + 3.13333e^{-005}\ \textit{Sliding distance}, \quad (1)$$

$$\textit{Wear rate of mono MMCs} = -0.023713 + 0.00555556\ \textit{Load} + \\ + 3.80556e^{-005}\ \textit{Sliding speed} + 2.95556e^{-005}\ \textit{Sliding distance}, \quad (2)$$

$$\textit{Wear rate of hybrid MMCs} = -0.0328241 + 0.00466667\ \textit{Load} + \\ + 3.13889e^{-005}\ \textit{Sliding speed} + 3.53333e^{-005}\ \textit{Sliding distance}. \quad (3)$$

The regression analysis has typically been employed to investigate the responses between the parameters. Test trials have been run to ensure that anticipated values are accurate, and graphical representations are used to compare experimentation results with predictions. In Fig. 6, the wear behaviour of base material, mono MMCs, and hybrid composites is depicted in response to expected and experimental values.

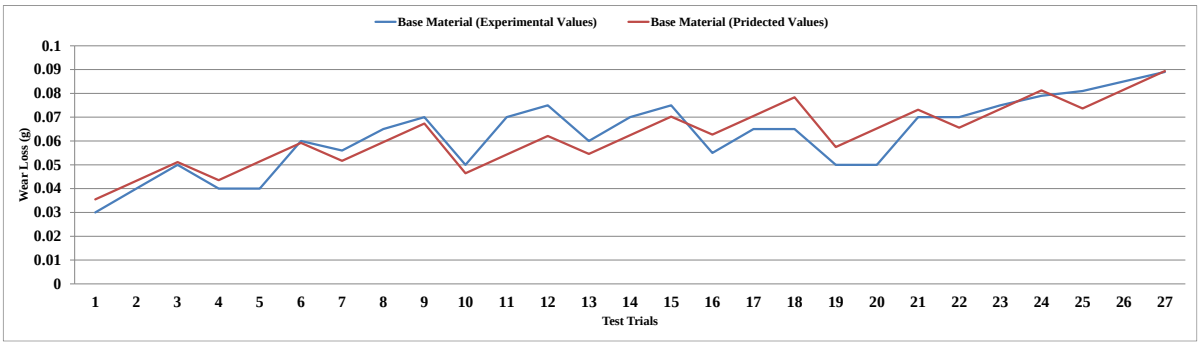

(a)

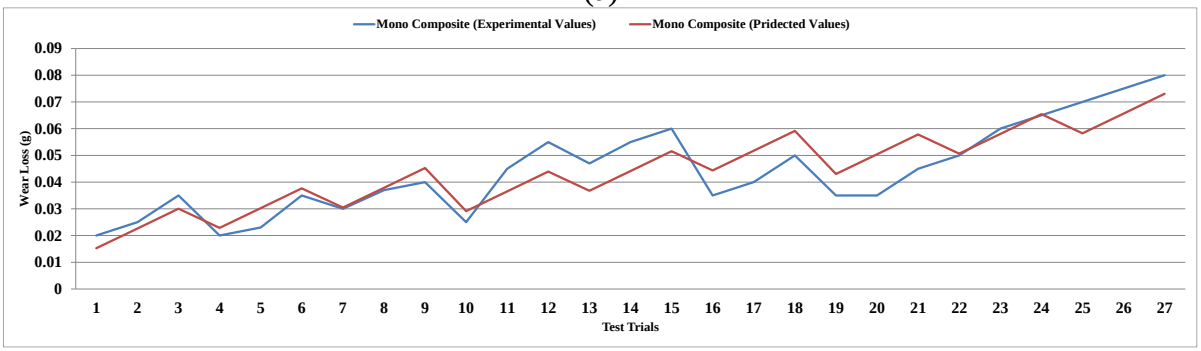

(b)

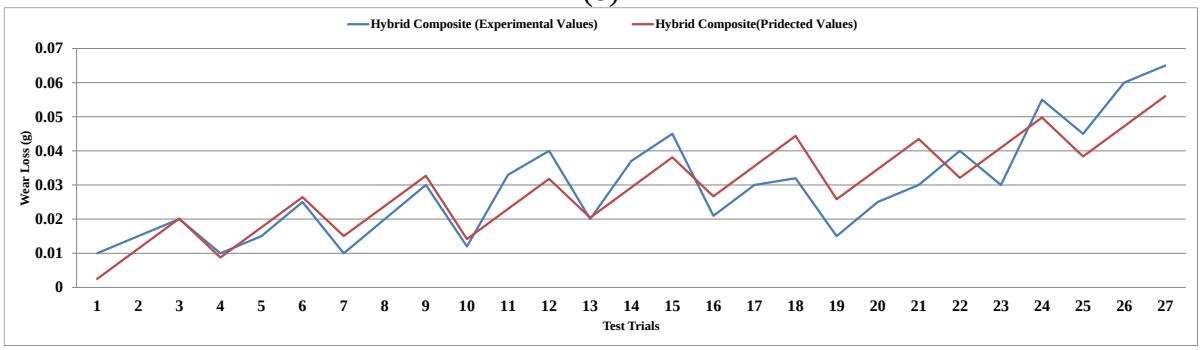

(c)

Fig. 6. Experimental vs. predicted values of wear loss for (a) monolithic alloy, (b) mono MMCs and (c) hybrid MMCs

The regression model's contour plots, are drawn and utilised to display the combined impact of the parameters used in the current inquiry. These graphs are typically used to show how the two parameters interact with one another. The optimal values of each parameter could be anticipated by analysing these plots [30]. Figures 7-9 display the contour graphs for the wear loss based on the independent factors for all the developed materials.

The results of wear behaviour in variations of wear factors with different material composition are shown in Fig. 7-9. It has been found that when load, speed and sliding distance are increased, wear loss also increases. Higher loads and faster speeds revealed considerable friction. As a result, a higher temperature was developed on the test sample surface. Brittleness has caused materials' hardness to decrease as a result, and the wear loss was increased. When there is increase in temperature, the link between the reinforcement and matrix gradually weakened, and the material softened [31]. The primary goal of the confirmatory trials was to determine the ideal ranges for the various process parameters that were chosen. Based on the Main Effects Plot (MEP) optimal values, confirmation tests were carried out (Fig. 5). Table 10 shows the parameters at the chosen levels. The results of the confirmatory experimental trials are reported in Table 11 and compared to experimental data

from OA. The outcome shows that for all composite materials, the computed errors are fewer than 10 %. This falls inside allowable bounds.

Table 10. Confirmatory test parameters with optimized values

Factors	Load, N	Sliding speed, rpm	Sliding distance, m
Optimized values for all the developed materials	5	100	250

Table 11. Confirmation test outcomes for all developed materials

Configuration	Parameters	Confirmatory test results	OA experimental results	Error, %
Base alloy (Al-7075)	Load (N): 5 Sliding speed (rpm): 100 Sliding distance (m): 250	0.030	0.029	3.33
Mono composite (10 % Al_2O_3)		0.020	0.019	5.00
Hybrid composite (10 % Al_2O_3 + 5 % SiC)		0.010	0.011	9.09

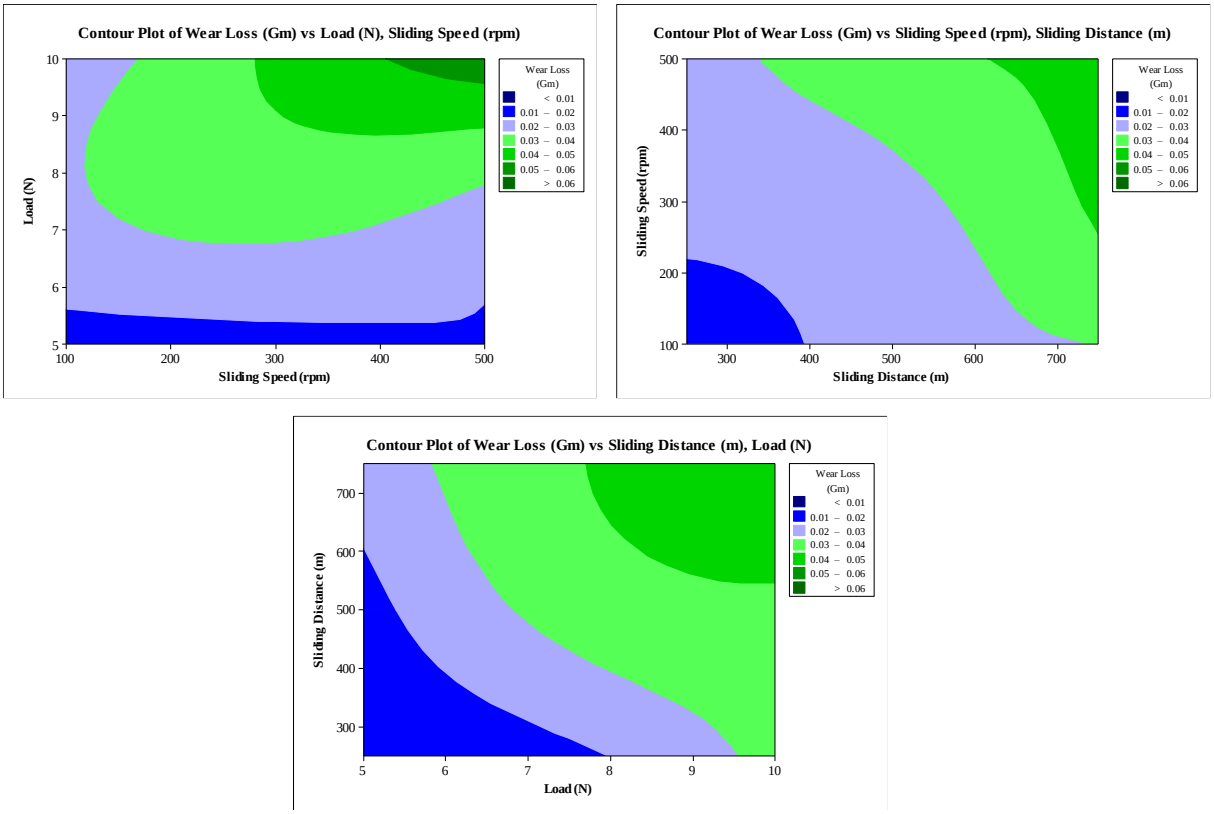

Fig. 7. Contour Plot of monolithic alloy

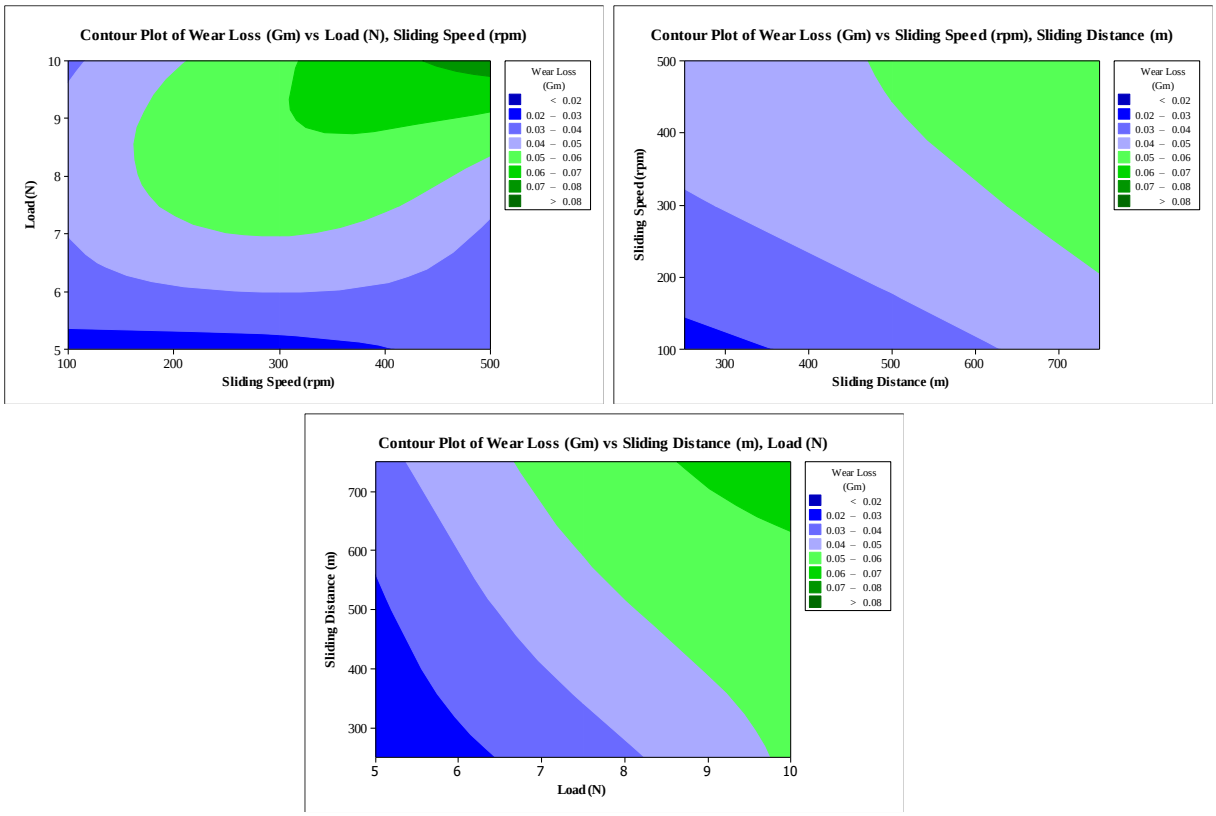

Fig. 8. Contour Plot of mono MMCs

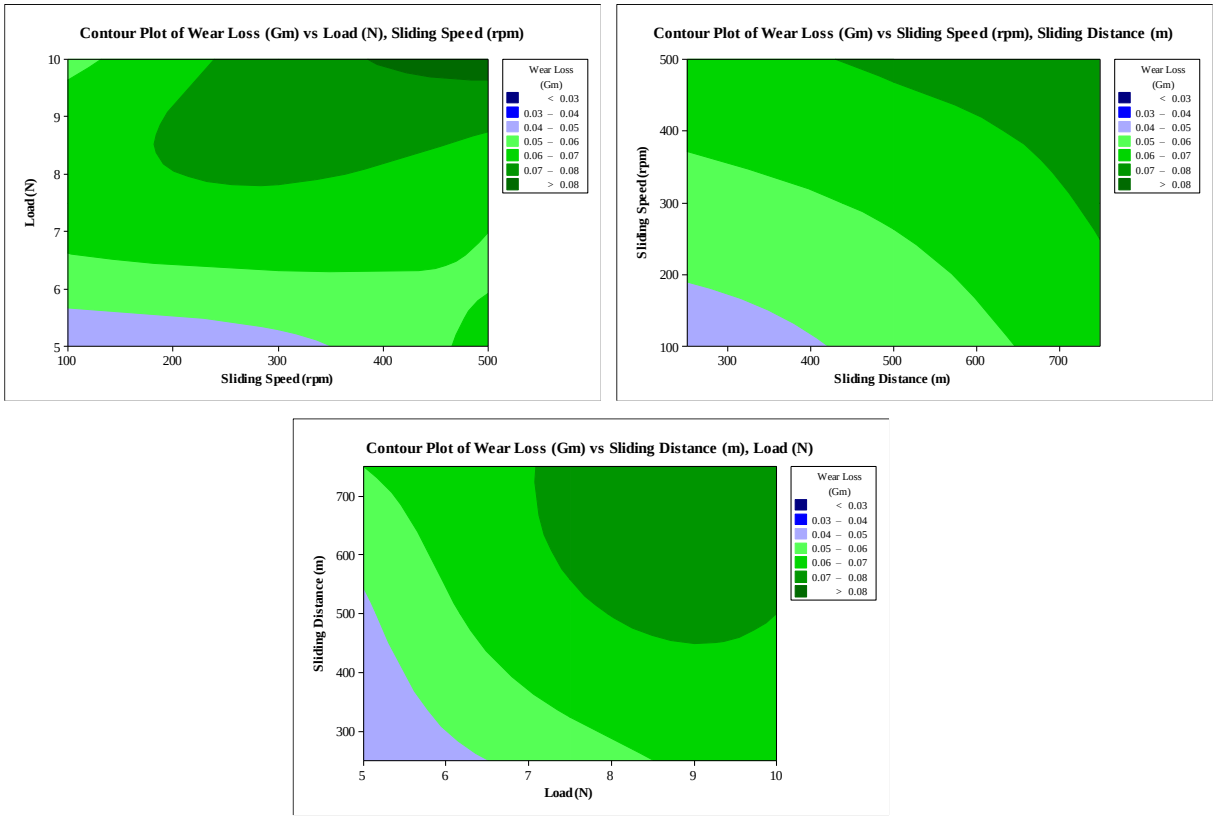

Fig. 9. Contour Plot of hybrid MMCs

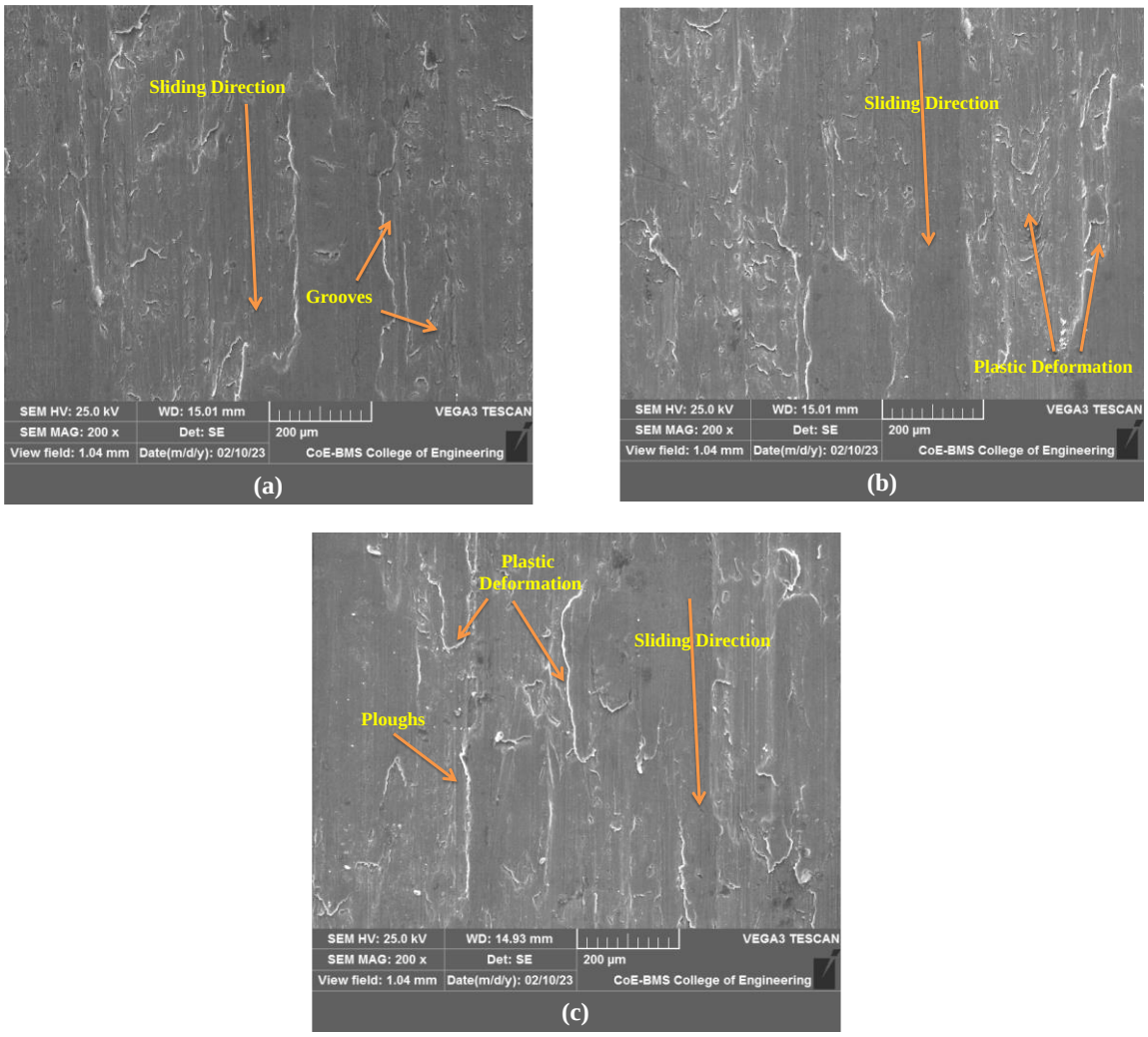

Fig. 10. Worn-out surface of (a) monolithic alloy, (b) mono MMCs and (c) hybrid MMCs

SEM analysis of the worn-out composites samples was done to analyse the wear characteristics of the MMCs. Typically, the MMCs' worn-out surface's properties will have an impact on the wear behaviour. Figure 10 shows a SEM image of a worn-out surface from matrix, mono, and hybrid composites that were evaluated under conditions of 10 N load, 500 rpm speed, and 1000 m sliding distance. The wear track that forms on the surface of the Al 7075, mono, and hybrid MMCs is clearly visible in the SEM pictures. Figure 10(a) depicts the basic alloy Al7075's worn-down surface. The image shows plastic deformation caused by the monolithic becoming less rigid at the interface temperature. Al7075 exhibited an adhesive wear mechanism at greater levels of stress, speed, and sliding distance. Without reinforcement, the image demonstrates with clarity how intense the wear is. It is concluded that the absence of reinforcements typically results in extensive plastic deformation of the matrix. Thus, the worn surface exhibits more material losses. Figure 10(b) shows a SEM image of an Al7075 composite with 1 % Al_2O_3 and more shallow grooves. Generally speaking, the wear resistance will be very high due to the existence of hard reinforcement. Moreover, the worn-out surface is rough due to ceramic particles that were exposed while the composite was being worn down during sliding on the steel disc. The abrasion on the composite surface caused by the hard particles being pulled out resulted in plastic deformation of the particles. It demonstrates that when Al_2O_3 particles were added, wear loss in the monolithic composite was reduced to a minimum. The SEM picture of the composite made of Al7075 with 1 % Al_2O_3 and 1 % SiC is shown in Fig. 10(c). Al_2O_3 and SiC particles

in this area boost wear resistance. When it is compared to the mono composite and base material, the image demonstrates that hybrid MMCs has a significantly rougher surface. The wear surfaces of the composite show many, deep grooves and voids. High reinforcement weight percentages result in high wear resistance. The addition of hard ceramic particles has been researched for its impact on the wear process, which provides a number of explanations for the exceptional wear resistance of hybrid MMCs. Due to the hard SiCp reinforcement undergoing chemical interactions during sliding, typically acts as a lubricant. This is especially true at high sliding speeds. MML's protection is seen to improve as the reinforcement content is increased. Several researchers [32–35] noted comparable results.

Figure 11 displays the results of an EDS analysis of base material, mono-composite, and hybrid composites. An EDS analysis of the mono composite surface depicted in Fig. 11(a) indicated the existence of oxygen ("O" peak) as a result of an oxidised layer, suggesting that the composite contains Al_2O_3 (aluminium oxide). Together with the mono reinforcing, the presence of a "Si" peak was noted in the developed hybrid composite (Fig. 11(b)). This demonstrates that SiC particles are present in the hybrid composite. The carbide particles have a significant impact on the wear behaviour of composite materials because, in contrast to mono composite and base materials, wear loss is decreased due to the existence of hard ceramic particulates. Several researchers [36–39] have reported similar results.

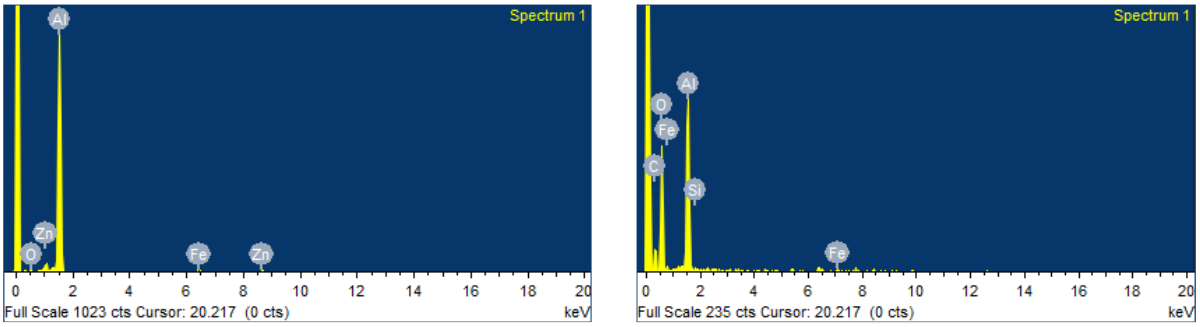

(a) (b)

Fig. 11. EDS analysis of (a) mono composites (Al7075 + 1% Al_2O_3) and (b) hybrid composites (Al7075 + 1% Al_2O_3 + 1% SiC)

Conclusions

The evaluation of Al-7075, mono composites (Al7075 + 1 % Al_2O_3), and hybrid MMCs (Al7075 + 1 % Al_2O_3 + 1 % SiC) revealed several significant aspects.

Using the stir casting technology, the monolithic alloy, mono, and hybrid composites were effectively produced in the current experiment. It was observed that adding more tough ceramic particles increased the material's hardness and tensile strength. In contrast to mono composites and aluminium alloy, hybrid MMCs exhibited improved tensile and hardness strength. It has been revealed that the inclusion of SiCp reinforcement produces hybrid MMCs materials that have excellent wear resistance when it is compared to base materials and mono MMCs. ANOVA study revealed that the applied load had a stronger influence on wear rate than sliding speed and the sliding distance. The correlation between the parameters and wear properties has been studied using Regression Analysis. R-Sq (R2), the coefficient of determination, was calculated and found to be within acceptable limits. According to the results of the confirmation test, the error associated with base material, mono, and hybrid MMCs is less than 10 %. In comparison to mono-composite and monolithic surfaces, worn-out hybrid composite surfaces exhibit high levels of abrasion wear, as shown by a SEM image. It's because the developed mono composites and hybrid composites contain strong ceramic reinforcement like nano sized Al_2O_3 and SiC content. According to EDS data, mono composite materials include nano sized Al_2O_3, while hybrid composite materials contain nano

sized Al_2O_3-SiC. According to the results of the confirmatory experiment test, the maximum error for hybrid MMCs was 9.09 %, but it was significantly lower for the other two compositions. This falls inside allowable limits.

References

1. Ganesh K, Hemachandra Reddy K, Sudhakar Babu S, Ravikumar M. Study on microstructure, tensile, wear, and fracture behavior of A357 by modifying strontium (Sr) and calcium (Ca) content. *Materials Physics and Mechanics*. 2023; 51(2): 128-139.
2. KumarV, Angra S, Singh S. Influence of rare earth elements on aluminium metal matrix composites: A review. *Materials Physics and Mechanics*. 2023; 51(2): 1-20.
3. Arunprasath K, Amuthakkannan P, Vijayakumar M, Sundarakannan R, Selwin M, Kavitha S, Lavish Kumar Singh. Effect of Mechanical Properties of AL7075/Mica Powder Hybrid Metal Matrix Composite. *Materials Physics and Mechanics*. 2023; 51(1): 142-150.
4. Kumar MSA, Kumar KCM, Prasad SLA. Experimental investigations on mechanical and Tribological properties of extruded Aluminium A356 - Al_2O_3 stir cast MMC. *Mater Today Proc.* 2018;5(1): 3044–3051.
5. Alhawari KS, Omar MZ, Ghazali MJ, Salleh MS, Mohammed MN. Wear properties of A356/Al_2O_3 metal matrix composites produced by semisolid processing. *Procedia Eng.* 2013;68: 186–192.
6. Sajjadi SA, Torabi Parizi M, Ezatpour HR, Sedghi A. Fabrication of A356 composite reinforced with micro and nano Al_2O_3 particles by a developed compocasting method and study of its properties. *J. Alloys Compd*. 2012;511: 226–231.
7. Ahmed KE, Nagesh BM, Raju BS, Drakshayani DN, Holla ASC. Studies on the effect of welding parameters for friction stir welded AA6082 reinforced with Aluminium oxide. *Mater Today Proc.* 2020;20: 108–119.
8. Prasad Reddy A, Vamsi Krishna P, Narasimha Rao R, Murthy NV. Silicon carbide reinforced Aluminium metal matrix Nano composites-a review. *Mater Today Proc.* 2017;4(2): 3959–3971.
9. Ghandvar H, Idris MH, Ahmad N Moslemi N. Microstructure development, mechanical and tribological properties of a semisolid A356/xSiCp composite. *J. Appl. Res Technol*. 2017;15(6): 533–544.
10. Amouri K, Kazemi S, Momeni A, Kazazi M. Microstructure and mechanical properties of Al-nano/micro SiC composites produced by stir casting technique. *Mater Sci. Eng. A.* 2016;674: 569–578.
11. Shivamurthy RC, Surappa MK. Tribological characteristics of A356 Al alloy SiCp composite discs. *Wear*. 2011;271(9-10): 1946–1950.
12. Iyengar SRS, Sethuramu D, Ravikumar M. Mechanical, Wear, and Fracture Behavior of Titanium Diboride (TiB_2) - Cerium Oxide (CeO_2) Reinforced Al-6061 Hot-rolled Hybrid Composites. *Frattura ed Integrità Strutturale*. 2023;63: 289-300.
13. Ghosh S, Sahoo P, Sutradhar G. Tribological Performance Optimization of Al-7.5 % SiCp Composites Using the Taguchi Method and Grey Relational Analysis. *J. Comp.* 2013;2013: 274527.
14. Ekka KK, Chauhan SR, Varun. Study on the sliding wear behaviour of hybrid aluminium matrix composites using Taguchi design and neural network. *J. Materials: Design and Applications.* 2016;230(2): 537–549.
15. Panwar RS, Pandey OP. Study of Wear Behavior of Zircon Sand-Reinforced LM13 Alloy Composites at Elevated Temperatures. *J. of Materi Eng and Perform.* 2013;22: 1765–1775.
16. Sharma P, Sharma S, Khanduja D. Production and some properties of Si3N4reinforced aluminium alloy composites. *Journal of Asian Ceramic Societies*. 2015;3(3); 352–359.
17. Suresh S, Gowd GH, Deva Kumar MLS. Experimental investigation on mechanical properties of Al 7075/Al_2O_3/Mg NMMC's by stir casting method. *Sadhana.* 2019;44(51): 1–10.

18. Bhaskar S, Kumar M, Patnaik A. Effect of Si3N4 Ceramic Particulates on Mechanical, Thermal, Thermo-Mechanical and Sliding Wear Performance of AA2024 Alloy Composites. *Silicon*. 2022;14: 239–262.
19. Sekar K. Mechanical and tribological properties of Al7475-SiCp composites by stir casting method and wear rate modeling using RSM. *Sadhana*. 2019;44: 129.
20. Ravikumar M, Suresh R. Study on mechanical and machinability characteristics of n-Al_2O_3/SiC-reinforced Al7075 composite by design of experiment technique. *Multiscale and Multidisciplinary Modeling, Experiments and Design*. 2018; https://doi.org/10.1007/s41939-023-00179-4.
21. Balakumar G. Fracture Behavior of Aluminum alloy Reinforced with Nano-ZrO2Metal Matrix Composite (NMMCs) by DMD Technique. *International Journal of NanoScience and Nanotechnology*, 2013; 4(2): 153–161.
22. Kavimani V, Gopal PM, Sumesh KR, Kumar NV. Multi Response Optimization on Machinability of SiC Waste Fillers Reinforced Polymer Matrix Composite Using Taguchi's Coupled Grey Relational Analysis. *Silicon*. 2020;14: 65–73.
23. Murali Mohan R, KempaiahUN, Manjunatha B, Madeva Nagaral, Auradi V. Processing and wear behavior optimization of B_4C and rice husk ash dual particles reinforced ADC12 alloy composites using Taguchi method. *Materials Physics and Mechanics*. 2022; 50(2): 304-318.
24. Dhanalakshmi S, Mohanasundararaju N, Venkatakrishnan PG, Karthik V. Optimization of friction and wear behaviour of Al7075-Al_2O_3-B_4C metal matrix composites using Taguchi method. *IOP Conf. Series: Materials Science and Engineering*. 2018;314: 012025.
25. Narasimha GB, Krishna MV, Sindhu R. Prediction of Wear Behaviour of Almg1sicu Hybrid MMC Using Taguchi with Grey Rational Analysis. *Procedia Engineering.* 2014;97: 555–562.
26. Radhika N. Fabrication of LM25/SiO_2 Metal Matrix Composite and Optimization of Wear Process Parameters Using Design of Experiment. *Tribology in Industry*. 2017; 39(1): 1–8.
27. Jafari F, Sharifi H, Saeri MR, Tayebi M. Effect of Reinforcement Volume Fraction on the Wear Behavior of Al-SiCp Composites Prepared by Spark Plasma Sintering. *Silicon*. 2018;10: 2473–2481.
28. Wakjira MW, Altenbach H, Perumalla JR. Analysis of CSN 12050 Carbon Steel in Dry Turning Process for Product Sustainability Optimization Using Taguchi Technique. *Journal of Engineering.* 2019;2019: 7150157.
29. Satyanarayana T, Rao PS, Krishna MG. Influence of wear parameters on friction performance of A356 aluminum - graphite/granite particles reinforced metal matrix hybrid composites. *Heliyon*. 2019;5(6): e01770.
30. Ashengroph M, Nahvi I, Amini J. Application of Taguchi Design and Response Surface Methodology for Improving Conversion of Isoeugenol into Vanillin by Resting Cells of Psychrobacter sp. CSW4. *Iranian Journal of Pharmaceutical Research*. 2013;12(3): 411–421.
31. Marigoudar RN, Sadashivappa K. Effect of reinforcement percentage on wear behavior of SiCp reinforced ZA43 alloy metal matrix composites. *Sci. Eng. Compos. Mater*. 2013;20(4): 311–317.
32. Gajakosh A, Keshavamurthy R, Vasanth Kumar R. Friction and Wear Characteristics of Hot-Rolled Al7075-TiO2-Graphite Hybrid Composites. *J. Inst. Eng. India Ser. D*. 2022.
33. Kumar D, Singh S, Angra S. Effect of reinforcements on mechanical and tribological behavior of magnesium-based composites: a review. *Materials Physics and Mechanics*. 2022;50(3): 439-458.
34. Chen W, Wenhui H, Zhao Z, He N, Xiuqing L. Mechanical properties and tribological characteristics of B4C-SiC ceramic composite in artificial seawater. *Journal of Asian Ceramic Societies*. 2021;9(4): 1495–1505.
35. Ünlü BS. Investigation of tribological and mechanical properties Al_2O_3-SiC reinforced Al composites manufactured by casting or P/M method. *Materials and Design.* 2008;29(10): 2002–2008.
36. Riquelme A, Rodrigo P, Escalera-Rodríguez MD, Rams J. Corrosion Resistance of Al/SiC Laser Cladding Coatings on AA6082. *Coatings*. 2020;10(673): 1–12.

37. Arif S, Alam T, Ansari AH, Shaikh MBN. Morphological characterization, statistical modelling and tribological behaviour of aluminum hybrid nanocomposites reinforced with micronano-silicon carbide. *Journal of Asian Ceramic Societies*. 2019;7(4): 434–448.
38. Matus K, Matula G, Pawlyta M, Krzysteczko-Witek J, Tomiczek B. TEM Study of the Microstructure of an Alumina/Al Composite Prepared by Gas-Pressure Infiltration. *Materials*. 2022;15(17): 6112.
39. Muraliraja R, Arunachalam R, Al-Fori I, Al-Maharbi M, Piya S. Development of alumina reinforced aluminum metal matrix composite with enhanced compressive strength through squeeze casting process. *J. Materials: Design and Applications*. 2019;233(3): 307–314.

THE AUTHORS

Ravikumar M.
e-mail: ravikumar.muk@gmail.com

Naik R.
e-mail: rudranaik.mech@bmsce.ac.in

Vinod B.R.
e-mail: vinod.vbr@gmail.com

Chethana K.Y.
e-mail: chethanaky.aer@bmsce.ac.in

Rammohan Y.S.
e-mail: ysrmohan.mech@bmsce.ac.in